ARTICLES

Predicting evolutionary patterns of mammalian teeth from development

Kathryn D. Kavanagh[1]†, Alistair R. Evans[1] & Jukka Jernvall[1,2]

One motivation in the study of development is the discovery of mechanisms that may guide evolutionary change. Here we report how development governs relative size and number of cheek teeth, or molars, in the mouse. We constructed an inhibitory cascade model by experimentally uncovering the activator–inhibitor logic of sequential tooth development. The inhibitory cascade acts as a ratchet that determines molar size differences along the jaw, one effect being that the second molar always makes up one-third of total molar area. By using a macroevolutionary test, we demonstrate the success of the model in predicting dentition patterns found among murine rodent species with various diets, thereby providing an example of ecologically driven evolution along a developmentally favoured trajectory. In general, our work demonstrates how to construct and test developmental rules with evolutionary predictability in natural systems.

A recurring promise of evolutionary developmental biology is the discovery of the mechanisms and rules that govern the production of the phenotypic variation available for natural selection[1–7]. In many cases, independent evolutionary acquisitions of morphological similarities have been linked to parallel changes in the genome[8–11], but selection may also produce the same phenotypic result in different evolutionary trials by altering different genes or interactions[12–15]. Whereas in the former cases gene-level or low-level rules may have predictive power across a broad range of taxa, in the latter cases models may have to be built on a higher level of organization. Regardless of the organizational levels invoked, explicit or inferred developmental rules with evolutionary relevance must be shown to favour specific evolutionary trajectories, and previous demonstrations have ranged from theoretical and computational models to selection and developmental experiments[1–7]. Advances in developmental genetics now allow us to identify mechanisms that may bias the production of phenotypic variation, which in part will help to move evolutionary developmental biology into the realm of a predictive science.

The mammalian dentition is a classic system in which developmental mechanisms have been used to explain variation in shape and size[16–22]. The timing of molar initiation during development has been extensively studied in primates, not least because molar proportions are used as a diagnostic feature in palaeontology. Differences in the timing of molar initiation, mineralization and eruption as well as in molar size and number have been linked to species-specific traits in diet, life history, maturation and brain size[23–26]. In addition, regulation of molar size and number continues to have medical relevance in connection with human third molars, or wisdom teeth, which are frequently surgically removed with a risk of complications[27].

Mammalian molars develop sequentially in an anterior to posterior direction (Fig. 1a), resembling the development of segmental structures, but it remains unknown how molar initiation or size is regulated along the tooth row. Mechanisms including available space in the jaw and inhibition between developing teeth have both been proposed to regulate molar initiation[21,22,25]. Because experimental evidence and mathematical modelling have implicated a balance of molecular signals activating and inhibiting the formation of teeth[28–30], here we examine whether inhibitory dynamics could explain the initiation and size of adjacent molars in mouse (*Mus musculus*) and whether these dynamics can account for aspects of evolutionary patterns of teeth.

Inhibitory dynamics of molar initiation

As in most eutherian mammals, mice have three molars that develop sequentially over several days[31]. The development of each individual tooth is punctuated by the formation of the epithelial signalling

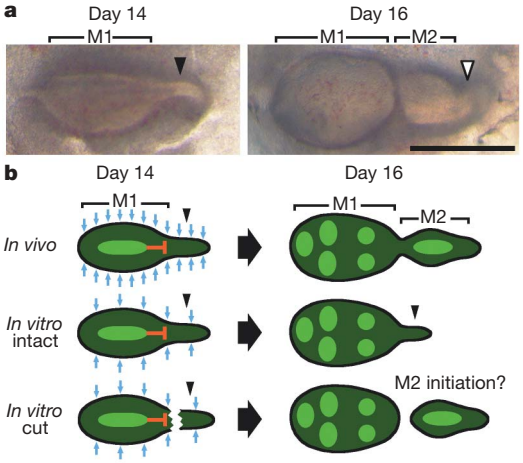

Figure 1 | Hypotheses on the sequential initiation and inhibition of mammalian cheek teeth. a, Mouse molars develop sequentially, and the dental lamina extending posteriorly (black arrowhead) from the developing M1 gives rise to M2 at day 16. M3 forms (white arrowhead) posterior to M2 about ten days later. **b**, In comparison with the situation *in vivo*, M1 development proceeds normally *in vitro* and the secondary enamel knots form at day 16 (bright green). In contrast, M2 initiation is delayed *in vitro*. We suggest that this delay is due to a decrease in mesenchymally secreted activators (blue arrows), whereas M1 continues to inhibit M2 normally. To test this, we cut the posterior tail that forms M2 from M1. Anterior is towards the left. Scale bar, 0.5 mm.

[1]Evolution & Development Unit, Institute of Biotechnology, PO Box 56 (Viikinkaari 9), FIN-00014 University of Helsinki, Finland. [2]Department of Ecology and Evolution, Stony Brook University, Stony Brook, New York 11794, USA. †Present address: School of Marine and Atmospheric Sciences, Stony Brook University, Stony Brook, New York 11794, USA.

centres, the enamel knots[28]. A primary enamel knot forms at the onset of the tooth crown development, followed by secondary enamel knots that appear at the future positions of major molar features, the cusps. Because mutations affecting the inhibition of enamel knots can have fused or extra cusps and molars[30], we postulate that the first developing molar could inhibit the development of subsequent molars, an effect that we also propose to be accentuated by culture conditions. In culture, although the first molar (M1) develops at essentially the same rate as that *in vivo*, posterior molars are frequently delayed by several days or never develop at all. The culture conditions, which involve the dissection of tooth germs from surrounding tissue, seem to disrupt the mesenchymal influence on the balance of activator and inhibitor molecules regulating molar development (Fig. 1b).

To test these ideas, we cultured lower first molar tooth germs from a mouse that expressed green fluorescent protein (GFP; fused with Cre-recombinase) in the Sonic Hedgehog (*Shh*) locus (hereafter called *ShhGFP* mice). In the developing tooth crown, *Shh* is first upregulated only in the cells of the enamel knots; later, during differentiation, *Shh* expression is detected in the enamel-secreting ameloblasts throughout the crown[28,32]. Because enamel knots are difficult to detect under normal culture conditions, the epifluorescence of *ShhGFP* mice allowed us to pinpoint the future positions of the molars and cusps *in vitro*, thereby permitting us to follow the sequential odontogenesis continuously (Fig. 2a). The *ShhGFP* construct is a *Shh*-null allele; we therefore cultured heterozygous *ShhGFP* molars. Similarly to a previous report on limb development[33], we found the tooth development and morphology of heterozygous *ShhGFP* mice to be normal. We also examined the development of wild-type molars, and the pattern of results remained essentially the same.

Using a standard Trowell culture system[34], we first cultured *ShhGFP* molars starting from embryonic day 14, at which time the M1 primary enamel knot has formed. We cultured both intact tooth germs and teeth in which we surgically separated the developing M1 from its posterior tail that is fated to give rise to the second (M2) and third (M3) molars (Figs 1 and 2a). Cultures were monitored daily, and the initiation of each tooth was reconstructed from time-lapse images (Fig. 2a). For the cultured intact tooth germs, the results show that only 11% of explants formed M2 enamel knots after two days in culture, a period equivalent to the timing of M2 initiation *in vivo* (Fig. 2b). Additional intact explants developed M2s during the subsequent days, and 54% of M2s were initiated by 12 days in culture (Fig. 2b). In contrast to this delayed initiation of M2 development, M1 development progressed at a fairly normal rate and all M1s had formed secondary enamel knots by three days into the culture (Fig. 2a), matching the rate of development *in vivo*[28]. The normal development of M1 implies that nutritional deficiency is unlikely to cause the delay in the posterior molars, but it supports the hypothesis of inhibition by M1 (Fig. 1b).

For the explants in which the tail had been cut off from the rest of the tooth germ, the results show that 98% of the separated tails formed M2s, with 68% of them occurring at the *in vivo* rate (Fig. 2b). Therefore, rather than inflicting irreversible damage on the small posterior bud, the separation seems to rescue M2 development from an inhibitory effect of M1. We interpret this result to also exclude an inhibitory gradient going through the jaw and teeth, increasing from anterior to distal, because in that case we would not expect the separation to rescue M2s. Furthermore, in almost half of the cut explants, M3 development was initiated, often before expected M3 initiation *in vivo* (Fig. 2c).

At the day 14 cap stage, when the M1 enamel knot has formed, M1 expresses the genes encoding several signalling molecules[28], including diffusible inhibitors. Of these, at least *ectodin* (also known as *Sostdc1* and *wise*, inhibitor of bone morphogenetic proteins (BMPs) and Wnts), *Bmp3* and *follistatin* (both encoding inhibitors of Activin A and BMPs) are strongly expressed in the enamel knot or anterior portion of the day 14 M1 (refs 30, 35, 36). Therefore, to test how an earlier release from inhibition affects posterior molars, we cut the posterior tails also at day 13, when the M1 primary enamel knot would only just be forming. These results show that posterior molar initiation was accelerated further: 90% of M2s were now initiated one day earlier than *in vivo* (Fig. 2b). The initiation of M3 development was also markedly accelerated (Fig. 2c). In addition, in one of the explants, a fourth molar (M4) formed seven days into the culture. We note that even though the tails giving rise to M3s were too small to be dissected from M2s, molar initiation was always sequential and in no case did we observe a simultaneous initiation of M2 and M3. Thus, M3 initiation is likely to be inhibited by M2 and, consequently, M4 is inhibited by M3.

Our results indicate that, as seems to occur with the regulation of fibroblast growth factors during tooth development[37], the balance

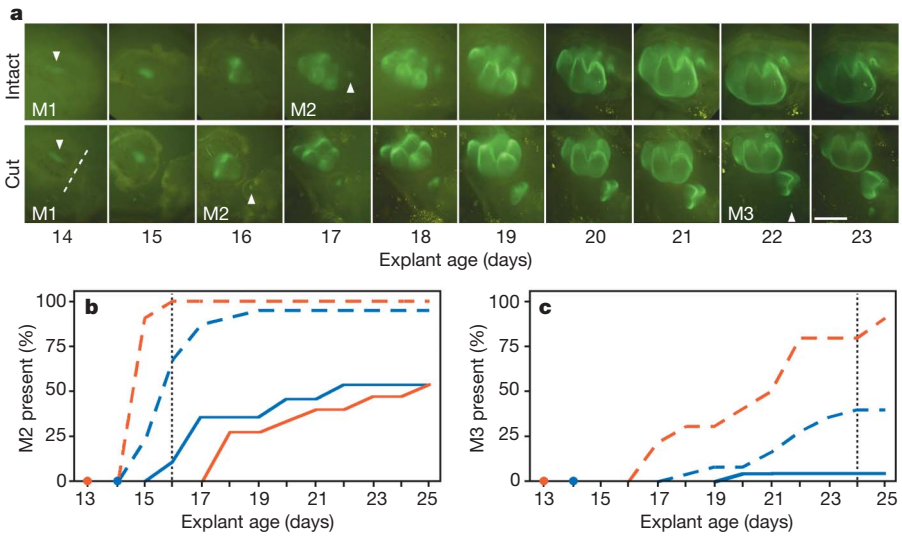

Figure 2 | Posterior molars are initiated earlier *in vitro* when separated from M1. **a**, The epifluorescence of cultured *ShhGFP* teeth allows daily monitoring of the enamel knots to test whether cutting the posterior tail (dashed line) accelerates molar initiation (white arrowheads). **b**, **c**, Cumulative percentage curves show that, in comparison with the intact explants (solid lines), the cut explants (dashed lines) at day 14 (blue) and day 13 (red) have an accelerated initiation of M2 (**b**) and M3 (**c**). *In vivo* M2 and M3 initiation times are marked with dotted vertical lines. Mann–Whitney *U*-tests on M2 and M3 age differences between intact and cut explants after 12 days of culture are all $P \leq 0.001$ (see Supplementary Information). $n = 28$ and $n = 25$ for day 14 intact and cut explants, respectively, and $n = 15$ and $n = 10$ for day 13 intact and cut explants, respectively. Scale bar, 0.5 mm.

between enamel knot activation and inhibition may be more important for tooth initiation than the absolute magnitude of signals themselves. Initially, the *in vitro* culture seems to decrease the level of mesenchymal activators required for M2 induction whereas removal of the inhibitory effect of M1 restores the inductive balance (Figs 1, 2). One obvious assumption linked to these interpretations is that culture conditions decrease mesenchymal activators required for enamel knot formation (Fig. 1b). To test this, we explored the effects of BMP4 and Activin A by using protein-releasing bead experiments. Both *Bmp4* and *activin βA* are intensely expressed in the mesenchyme at the onset of primary enamel knot formation, and both have been implicated as mediators of epithelial–mesenchymal induction events leading to the formation of enamel knots[30,36,38–40]. We placed beads releasing BMP4 or Activin A immediately distally to intact day 14 tooth germs. The results show that both molecules are individually able to accelerate the formation of M2s, although not to the extent that separation from M1 achieved (Fig. 3).

Taken together, our experimental results suggest that the initiation timing of posterior molars depends on previous molars through a dynamic balance between intermolar inhibition and mesenchymal activation. Because of the importance of molar size in evolution[6,16–29], we next explored how these developmental dynamics might bias the production of phenotypic variation available for natural selection.

Molar initiation and size

To link our results for the process of molar initiation to morphological patterns, we measured from our experiments how tooth size is affected by changes in tooth initiation (see Methods and Supplementary Information). The results show that the removal of inhibition on posterior molars results not only in earlier tooth initiation but also in larger posterior teeth. After 12 days of culture, M2s in the cut explants were twice the size of M2s in the intact explants (cut versus intact day 14 means are 0.27 and 0.13 mm^2, $P < 0.001$, and day 13 means are 0.23 and 0.11 mm^2, $P < 0.001$; Mann–Whitney *U*-tests). Furthermore, the cut explant M2s are larger not only as a result of earlier initiation but also because they grow faster (see Supplementary Information). In contrast, M1 sizes have marginally decreased in the cut explants, suggesting that dissection caused disruption and also that inhibition is always from anterior to posterior (cut versus intact day 14 means are 0.57 and 0.67 mm^2, $P = 0.027$, and day 13 means are 0.39 and 0.46 mm^2, $P = 0.123$; Mann–Whitney *U*-tests). Nevertheless, in comparison with the intact explants, both the day 13 and day 14 cut explants produced 15–38% more 'tooth', measured as the sum of the molar surface areas ($P = 0.005$–0.012; Mann–Whitney *U*-tests).

In the intact day 13 explants, the initiation of posterior molars was delayed in comparison with that of intact day 14 explants (Fig. 2b, c) and the M1s were also smaller, perhaps because of decreased mesenchymal activation that limited development at this earlier stage. Despite this typical retardation of day 13 tooth development *in vitro* (J. Jernvall and K. D. Kavanagh, unpublished observations), sizes of the day 13 cut explant M2s matched, and that of the M3s exceeded, the sizes of corresponding teeth from the day 14 cut explants (Fig. 4a; see Supplementary Information). The earlier separation from M1 therefore seems to lead to a tendency in which molar sizes become more equal (Fig. 4a). Whereas, for example, the day 14 M3s could in principle catch up with the day 13 M3s, this would require the former to grow more than twice as long as the latter. We consider this situation unlikely because in our cultures the onset of mineralization seemed to be the same in both the day 13 and day 14 cut explants.

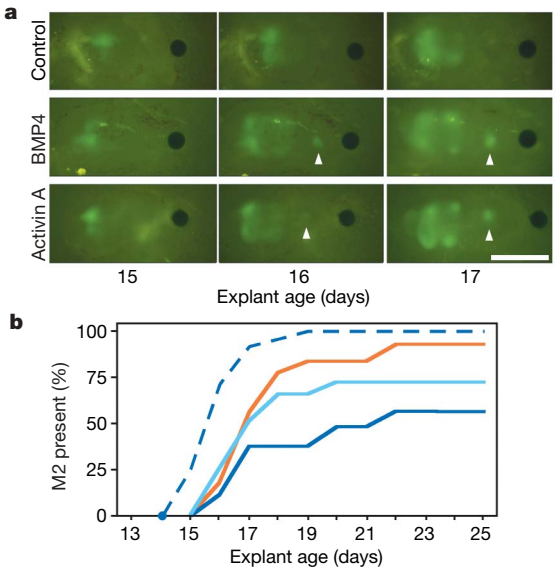

Figure 3 | Initiation of posterior molars can be stimulated by mesenchymal activators. **a**, Protein-releasing beads were placed posteriorly to day 14 explants and the initiation of M2s was monitored (white arrowheads). **b**, Both BMP4- (light blue line) and Activin A- (orange line) releasing beads accelerate M2 initiation, falling between the intact (solid blue line) and cut explants (dashed blue line). Mann–Whitney *U*-tests on M2 age differences between protein and control explants after 12 days of culture are $P = 0.122$ ($n = 16$) for BMP4 and $P = 0.014$ ($n = 19$) for Activin A explants (see Supplementary Information). Scale bar, 0.5 mm.

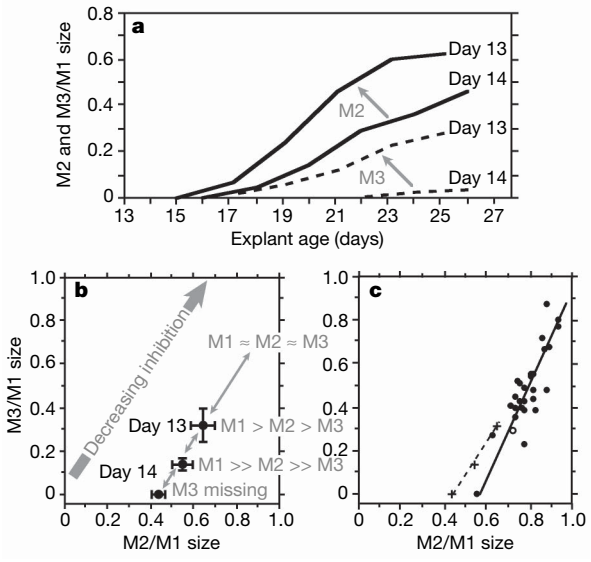

Figure 4 | From molar initiation to predicting molar proportions in murine species. **a**, Removal of inhibition results in earlier initiation and more equal-sized posterior molars. **b**, Changes in inhibition provide a trajectory through the morphospace in which more equal-sized molars are found with low inhibition (day 13 explants; error bars denote s.e.m). In contrast, increasing inhibition (day 14 explants) leads to smaller posterior molars and eventually the lack of M3. **c**, The molar proportions of 29 species of murine rodents (black circles; *Mus musculus* is marked with an open circle) fall close to the experimental data (crosses and dashed line). We note the lack of M3 when M2 is about half the size of M1, in both the experimental and the macroevolutionary data. For the experimental data, the slope drawn through the means of day 14 and day 13 molar sizes is 1.848 and the intercept is −0.833. When the 12 cut explants without M3s (all except one were day 14) are plotted separately (**b**), the resulting reduced major axis regression slope is 1.519 and the intercept is −0.673. When M1 sizes just before they reach their asymptotic sizes are used, approximating the growth stage of measured M2s and M3s, the reduced major-axis regression slope is 2.024 and the intercept is −0.997. For the macroevolutionary data (**c**), the reduced major-axis regression slope is 2.150 and the intercept is −1.219 ($r^2 = 0.740$). For details see Supplementary Information.

An inhibitory cascade model

The inhibitory dynamics (Figs 2, 3) and shifting molar proportions (Fig. 4a) are indicative of an inhibitory cascade, or a 'ratchet' in which subsequently developing teeth are cumulatively affected by previous developmental events. The inhibitory cascade can be formalized as a simple high-level model in which a balance between activation and inhibition results in equal-sized molars (M1 ≈ M2 ≈ M3) and increasing inhibition has a cumulative effect on the posterior teeth giving a distinct M1 > M2 > M3 pattern (Fig. 4b). The relative molar sizes determined by the model can be stated as $1 + [(a - i)/i](x - 1)$, in which, at each molar position (x), tooth size results from the relative strengths of activators (a) and inhibitors (i). As a result of the ratcheting nature of the inhibition, a change in inhibition (or activation) affects the relative size of M3 more than that of M2 (Fig. 4b). Nevertheless, molars have shared covariance patterns, so the relative size of adjacent teeth allows one to predict the presence and size of additional teeth. For example, M3s are missing when M2 size falls below half that of M1 (Fig. 4b). Conversely, our case of M4 occurred when the size of M3 equalled that of M2 (Supplementary Information), perhaps indicating that the evolution of supernumerary teeth is most likely when tooth activation and inhibition are in balance.

A macroevolutionary test of the model

Because our model makes broad predictions about the relative sizes of individual teeth, to test the model we focused on a sample of 29 species of murine rodents covering a wide spectrum of ecological adaptations and phylogenetic lineages representative of the entire subfamily[41,42] (Supplementary Information). Tooth rows were digitized with a high-resolution laser scanner and the molar crown areas were measured with the MorphoBrowser database containing the three-dimensional tooth scans[42].

The basic prediction from the experiments is that with an increase in relative size of M2, M3 should increase more. The results show that molar proportions follow this expectation closely (Fig. 4c), although the macroevolutionary patterns seem to show a slightly greater increase in posterior molars than the experimental prediction (Fig. 4c). We suspect that this is because our developmental data were derived from cultured teeth *in vitro* in which M1 was near mineralization whereas M2 and especially M3 could grow further, increasing their relative sizes. Indeed, when ante-asymptotic M1 sizes are used for the experimental data, the slopes of the molar size relationships are very similar between the experiments (2.02) and species (2.15). Conversely, in our molar diversity data, we have one species, golden-bellied water rat (*Hydromys chrysogaster*), which lacks M3 altogether. Matching the prediction from mouse explants lacking M3s, M2 in *Hydromys* is about half the size of M1 (Fig. 4c). Thus, despite the limitations of *in vitro* cultures (uncut M3s and incomplete differentiation), these results may implicate the inhibitory cascade in regulating tooth proportions.

Next, to test how closely the macroevolutionary data follow the explicit prediction of the inhibitory cascade model $1 + [(a - i)/i](x - 1)$, we first calculated the predicted sizes of M3s on the basis of the relative size of M2s (see Fig. 5a and Methods). Both the slope (2.0) and the intercept (−1.0) of the model prediction are within the 95% confidence intervals of the macroevolutionary data. To examine further the consistency of the tooth-to-tooth inhibitory relay in our data, we generated a random relay model, in which the strength of inhibition changed between teeth, by randomly reshuffling the M2-based predictions of M3 sizes 1,000 times (see Fig. 5a, Methods and Supplementary Information). The results show that whereas the random relay still produces correlated variation between relative M2 and M3 sizes (because, for example, it is unlikely that a large M2 is followed by a very small M3), its predictions are not congruent with our macroevolutionary data or model (Fig. 5a and Supplementary Information). We interpret these results as further implicating the inhibitory cascade as a 'ratchet' generating predictable size differences along the molar row.

One phenotypic outcome of the ratchet is the high variability of M3, a result that agrees well with data from populations and species[18–21,43,44]. Whereas the high variability of M3 has been linked to available space in the jaw and difficulty in measuring small M3s, the inhibitory cascade may provide null expectations for M3 variability. Another phenotypic result specific to the model is that M2 makes up roughly one-third of total molar area, irrespective of molar proportions ($M2/(M1 + M2 + M3) = (a/i)/[1 + a/i + (2a/i - 1)] = 1/3$; see Methods). This is noteworthy because previous studies have found this relationship in primates[45], suggesting that the inhibitory cascade may be expected to apply across mammalian orders.

Even though we have shown here how the inhibitory cascade can be used to account for the evolutionary diversity of molar proportions, ecological and functional factors are still likely to have an indirect function in these differences. For example, previous analyses have shown that the overall crown complexity of rodent molars closely reflects the species-specific diets[42]. High crown-feature complexity is associated with herbivory, whereas simpler, smaller crowns are found in animal-eating taxa[42]. In our diversity data, the highly derived species with either specialized animal or fibrous-vegetation diets are plotted at the far ends of the molar-proportion spectrum (Fig. 5b). In other words, herbivorous murine species have more equal-sized teeth, whereas more faunivorous species, such as *Hydromys* (Fig. 5b), have progressively more reduced distal teeth. In comparison with dental complexity[42], however, molar proportions seem not to be a measure of diet across mammalian orders because, for example, many herbivorous primates have progressively larger distal molars. We propose that molar proportions may not reflect function itself but may manifest the way in which development, by affecting the variational properties of teeth, responds to selection on functional features such as complexity and overall size.

Whereas our model predicts evolutionary change based on development, these predictions should not be taken as constraints on evolution. One clear exception is herbivorous arvicoline rodents (voles), in which the anterior part of their M1 is greatly elongated

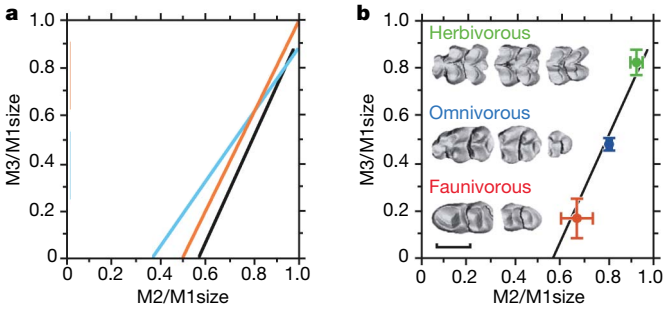

Figure 5 | The inhibitory cascade and the ecological context of murine dental diversity. a, From the macroevolutionary data (black line), the M2/M1 size was used to calculate the predicted M3/M1 size with the inhibitory cascade model (orange line; examples of molar proportions: M1 = M2 = M3; M1 > M2 > M3; M1 ≫ M2 ≫ M3). The random relay prediction illustrated (blue line: M1 = M2 > M3; M1 > M2 = M3; M1 ≫ M2 > M3), for which randomized M2/M1 sizes were used to predict M3/M1 sizes, is the mean of reduced major axis regressions performed on each of 1,000 random simulations. All correlations, slopes and intercepts of the diversity data and the prediction of the inhibitory cascade model are significantly different from those of the 1,000 random relays ($P = 0.005$ to $P < 0.001$). **b**, The most equal molar proportions are found in herbivorous taxa and the least equal in faunivorous taxa, indicating that the inhibitory-cascade-influenced phenotypic change is under the control of ecology. The three examples of molar rows are scaled to body size (scale bar, 0.01 of body length) and are for *Mallomys rothschildi* (herbivore, $n = 2$), *Mus musculus* (omnivore, $n = 22$) and *Hydromys chrysogaster* (faunivore, $n = 3$), anterior towards the left. Error bars denote s.e.m. For details see Supplementary Information.

(refs 28, 46). This change can be considered a developmental novelty in which the M1 extension is allowed because there are no premolars in the anterior dental diastema. Nevertheless, we postulate a general situation in which any developmentally derived rule would predict that organisms should most often fall on the developmentally favoured evolutionary trajectory (Figs 4 and 5). In the inhibitory cascade, for example, many Old World primates and ungulates have a weak inhibitory cascade resulting in large distal molars ($M1 < M2 < M3$), but are still predicted to fall along the predicted trajectory. In contrast, other kinds of developmental change would be required for invasion of other parts of the morphospace. For example, evolving $M1 < M2 > M3$ proportions can be predicted to require a combination of low inhibition and specific early arrest of M3 development. However, for murine molars, the inhibitory cascade seems to have sufficed when murine rodents, the most taxonomically diverse mammalian group living, radiated into multiple adaptive zones.

Conclusions

The inhibitory cascade model is an activator–inhibitor network-derived model that allows the prediction of evolutionary paths in a given selective environment. These kinds of mechanistic model differ from classical correlation-based approaches (for example, genetic covariance) because the developmental mechanism is identified and there is greater conceptual continuity from genotype to phenotype[3]. To this end, the exact genetic underpinnings of the inhibitory cascade model remain to be identified. Whereas possible molecular level candidates include signalling molecules (and their inhibitors) such as BMPs, Activin A (Fig. 3) and Ectodysplasin[47], and transcription factors such as Pax9 (ref. 48), the inhibitory cascade may or may not be centred on the same genes in every species. Ultimately, with many more than 500 extant species and divergence times extending from the Pleistocene through to the middle Miocene[41], murine rodents may provide excellent tests for the generality of high-level and low-level developmental rules. For this task, we would argue that the best tests of usefulness of identified developmentally derived rules are both the generality of the rule's use in other systems or taxa and the ability to demonstrate how development matters in explaining the evolution of phenotypes.

Because activator–inhibitor networks are a common mechanism in development, we suggest that inhibitory cascade-derived rules may apply in explaining the size relationships in adjacent organs beyond tooth development, particularly in other systems with sequentially developing organs or repeating elements. In insects, competition between developing body parts has been shown to affect the evolution of morphology[2,5], and the inhibitory cascade may also be understood as a form of sequential competition between adjacent organs. In teeth, our model resolves long-standing debates about the regulation of individual molar initiation and size, highlighting the essential role of inhibitors in shaping the entire dental system. Furthermore, our strategy of using the experimentally defined logic of organ systems to develop high-level testable models for predicting morphological evolution provides a blueprint for further exploration of evolutionary predictability in natural systems.

METHODS SUMMARY

Lower molar tooth germs were dissected from heterozygous *ShhGFP* mouse embryos[33] at day 13 or 14 after fertilization, as described previously[30,34]. Posterior tails (giving rise to M2 and M3) of developing M1s were separated, and both pieces were cultured a short distance from each other. Explants were photographed daily from initiation to day 12 of culture, and the molar initiation date was determined on the basis of the first visible epifluorescence marking the formation of each primary enamel knot. Recombinant protein beads[30,34] were placed on the posterior end of day 14 tooth germs. Tooth rows of 29 murine rodent species, representing the range of diets across the phylogeny within the subfamily, were scanned with a laser scanner and entered into the MorphoBrowser database (http://morphobrowser.biocenter.helsinki.fi/) as described previously[42]. Two-dimensional crown areas were measured from images of 61 explants and scans of 29 species. For all measures, statistical differences between groups were tested by using Mann–Whitney *U*-tests, each with two-tailed exact significance levels, performed in SPSS version 11.0 (SPSS Inc.). Model randomizations and calculations of reduced major-axis regressions[49] were performed in a custom Visual Basic 6.0 program (Microsoft Corp.) and additional calculations of reduced major-axis regressions were performed in PAST (http://folk.uio.no/ohammer/past/index.html) (see Supplementary Information).

Full Methods and any associated references are available in the online version of the paper at www.nature.com/nature.

Received 20 April; accepted 7 August 2007.

1. Alberch, P. & Gale, E. A. A developmental analysis of an evolutionary trend: Digital reduction in amphibians. *Evol. Int. J. Org. Evol.* **39,** 8–23 (1985).
2. Nijhout, H. F. & Emlen, D. J. Competition among body parts in the development and evolution of insect morphology. *Proc. Natl Acad. Sci. USA* **95,** 3685–3689 (1998).
3. Wagner, G. P., Chiu, C.-H. & Laubichler, M. Developmental evolution as a mechanistic science: the inference from developmental mechanism to evolutionary processes. *Am. Zool.* **40,** 819–831 (2000).
4. Salazar-Ciudad, I. & Jernvall, J. How different types of pattern formation mechanisms affect the evolution of form and development. *Evol. Dev.* **6,** 6–16 (2004).
5. Emlen, D. J., Hunt, J. & Simmons, L. W. Evolution of sexual dimorphism and male dimorphism in the expression of beetle horns: phylogenetic evidence for modularity, evolutionary lability, and constraint. *Am. Nat.* **166,** 42–68 (2005).
6. Polly, P. D. Development and phenotypic correlations: the evolution of tooth shape in *Sorex araneus*. *Evol. Dev.* **7,** 29–41 (2005).
7. Brakefield, P. M. & Roskam, J. C. Exploring evolutionary constraints in a task for an integrative evolutionary biology. *Am. Nat.* **168,** 4–13 (2006).
8. Colosimo, P. F. *et al.* Widespread parallel evolution in sticklebacks by repeated fixation of Ectodysplasin alleles. *Science* **307,** 1928–1933 (2005).
9. Protas, M. E. *et al.* Genetic analysis of cavefish reveals molecular convergence in the evolution of albinism. *Nature Genet.* **38,** 107–111 (2006).
10. Prud'homme, B. *et al.* Repeated morphological evolution through *cis*-regulatory changes in a pleiotropic gene. *Nature* **440,** 1050–1053 (2006).
11. Shapiro, M. D., Bell, M. A. & Kingsley, D. M. Parallel genetic origins of pelvic reduction in vertebrates. *Proc. Natl Acad. Sci. USA* **103,** 13753–13758 (2006).
12. True, J. & Haag, E. S. Developmental system drift and flexibility in evolutionary trajectories. *Evol. Dev.* **3,** 109–119 (2001).
13. Abouheif, E. & Wray, G. A. Evolution of the gene network underlying wing polymorphism in ants. *Science* **297,** 249–252 (2002).
14. Kawasaki, K., Suzuki, T. & Weiss, K. M. Phenogenetic drift in evolution: the changing genetic basis of vertebrate teeth. *Proc. Natl Acad. Sci. USA* **102,** 18063–18068 (2005).
15. Tanaka, M. *et al.* Developmental genetic basis for the evolution of pelvic fin loss in the pufferfish *Takifugu rubripes*. *Dev. Biol.* **281,** 227–239 (2005).
16. Bateson, W. *Materials for the Study of Variation, Treated with Special Regard to Discontinuity in the Origin of Species* (Macmillan, London, 1894).
17. Butler, P. M. Studies of the mammalian dentition. Differentiation of the post-canine dentition. *Proc. Zool. Soc. London (B)* **109,** 1–36 (1939).
18. Kurtén, B. On the variation and population dynamics of fossil and recent mammal populations. *Acta Zool. Fenn.* **76,** 1–122 (1953).
19. Van Valen, L. Growth fields in the dentition of *Peromyscus*. *Evol. Int. J. Org. Evol.* **16,** 272–277 (1962).
20. Gould, S. J. & Garwood, R. A. Levels of integration in mammalian dentitions: an analysis of correlations in *Nesophontes micrus* (Insectivora) and *Oryzomys couesi* (Rodentia). *Evol. Int. J. Org. Evol.* **23,** 276–300 (1969).
21. Sofaer, J. A., Bailit, H. L. & MacLean, C. J. A developmental basis for differential tooth reduction during Hominid evolution. *Evol. Int. J. Org. Evol.* **25,** 509–517 (1971).
22. Osborn, J. W. in *Development, Function and Evolution of Teeth* (eds Butler, P. M. & Joysey, K. A.) 171–201 (Academic, London, 1978).
23. Smith, B. H. Dental development and the evolution of life-history in Hominidae. *Am. J. Phys. Anthropol.* **8,** 157–174 (1991).
24. Godfrey, L. R., Samonds, K. E., Jungers, W. L. & Sutherland, M. R. in *Primate Life Histories and Socioecology* (eds Kappeler, P. M. & Pereira, M. E.) 177–203 (Univ. of Chicago Press, Chicago, 2003).
25. Boughner, J. C. & Dean, M. C. Does space in the jaw influence the timing of molar crown initiation? A model using baboons (*Papio anubis*) and great apes (*Pan troglodytes*, *Pan paniscus*). *J. Hum. Evol.* **46,** 253–275 (2004).
26. Macchiarelli, R. *et al.* How Neanderthal molar teeth grew. *Nature* **444,** 748–751 (2006).
27. Silvestri, A. R. Jr & Singh, I. The unresolved problem of the third molar: Would people be better off without it? *J. Am. Dent. Assoc.* **134,** 450–455 (2003).
28. Jernvall, J., Keränen, S. V. E. & Thesleff, I. Evolutionary modification of development in mammalian teeth: Quantifying gene expression patterns and topography. *Proc. Natl Acad. Sci. USA* **97,** 14444–14448 (2000).

29. Salazar-Ciudad, I. & Jernvall, J. A gene network model accounting for development and evolution of mammalian teeth. *Proc. Natl Acad. Sci. USA* **99,** 8116–8120 (2002).
30. Kassai, Y. *et al.* Regulation of mammalian tooth cusp patterning by Ectodin. *Science* **309,** 2067–2070 (2005).
31. Gaunt, W. A. An analysis of the growth of the cheek teeth of the mouse. *Acta Anat.* **54,** 220–259 (1963).
32. Gritli-Linde, A. *et al.* Shh signaling within the dental epithelium is necessary for cell proliferation, growth and polarization. *Development* **129,** 5323–5337 (2002).
33. Harfe, B. D. *et al.* Evidence for an expansion-based temporal Shh gradient in specifying vertebrate digit identities. *Cell* **118,** 517–528 (2004).
34. Sahlberg, C., Mustonen, T. & Thesleff, I. Explant cultures of embryonic epithelium: Analysis of mesenchymal signals. *Methods Mol. Biol.* **188,** 373–382 (2002).
35. Åberg, T., Wozney, J. & Thesleff, I. Expression patterns of bone morphogenetic proteins (Bmps) in the developing mouse tooth suggest roles in morphogenesis and cell differentiation. *Dev. Dyn.* **210,** 383–396 (1997).
36. Wang, X. P. *et al.* Modulation of activin/bone morphogenetic protein signaling by follistatin is required for the morphogenesis of mouse molar teeth. *Dev. Dyn.* **231,** 98–108 (2004).
37. Klein, O. D. *et al.* Sprouty genes control diastema tooth development via bidirectional antagonism of epithelial–mesenchymal FGF signaling. *Dev. Cell* **11,** 181–190 (2006).
38. Ferguson, C. A. *et al.* Activin is an essential early mesenchymal signal in tooth development that is required for patterning of the murine dentition. *Genes Dev.* **12,** 2636–2649 (1998).
39. Jernvall, J., Åberg, T., Kettunen, P., Keränen, S. & Thesleff, I. The life history of an embryonic signaling center: BMP-4 induces p21 and is associated with apoptosis in the mouse tooth enamel knot. *Development* **125,** 161–169 (1998).
40. Plikus, M. V. *et al.* Morphoregulation of teeth: modulating the number, size, shape and differentiation by tuning Bmp activity. *Evol. Dev.* **7,** 440–457 (2005).
41. Jansa, S. A., Barker, F. K. & Heaney, L. R. The pattern and timing of diversification of Philippine endemic rodents: Evidence from mitochondrial and nuclear gene sequences. *Syst. Biol.* **55,** 73–88 (2006).
42. Evans, A. R., Wilson, G. P., Fortelius, M. & Jernvall, J. High-level similarity of dentitions in carnivorans and rodents. *Nature* **445,** 78–81 (2007).
43. Garn, S. M., Lewis, A. B. & Kerewsky, R. S. Third molar agenesis and size reduction of the remaining teeth. *Nature* **200,** 488–489 (1963).
44. Polly, P. D. Variability in mammalian dentitions: size-related bias in the coefficient of variation. *Biol. J. Linn. Soc.* **64,** 83–99 (1998).
45. Lucas, P. W., Corlett, R. T. & Luke, D. A. Sexual dimorphism of tooth size in anthropoids. *Hum. Evol.* **1,** 23–29 (1986).
46. Guthrie, R. D. Variability in characters undergoing rapid evolution, an analysis of *Microtus* molars. *Evol. Int. J. Org. Evol.* **19,** 214–233 (1965).
47. Kangas, A. T., Evans, A. R., Thesleff, I. & Jernvall, J. Nonindependence of mammalian dental characters. *Nature* **432,** 211–214 (2004).
48. Kist, R. *et al.* Reduction of *Pax9* gene dosage in an allelic series of mouse mutants causes hypodontia and oligodontia. *Hum. Mol. Genet.* **14,** 3605–3617 (2005).
49. Sokal, R. R. & Rohlf, F. J. *Biometry* (Freeman, New York, 1995).

Supplementary Information is linked to the online version of the paper at www.nature.com/nature.

Acknowledgements We thank C. K. Chapple, G. Evans, M. Fortelius, I. Salazar-Ciudad, M. Mikkola, I. Thesleff, G. P. Wilson and P. C. Wright for comments, discussions and support with this work; P. Munne, M. Mäkinen, E. Penttilä, I. Pljusnin, R. Santalahti and R. Savolainen for technical help; M. Hyvönen for activin A recombinant protein; C. Tabin and A. Gritli-Linde for the *ShhGFPCre* mice; and the following museum curators and collection managers for loans: O. Grönwall, R. Asher, M. Hildén and I. Hanski. This study was supported by the Academy of Finland.

Author Contributions K.D.K. and J.J. conceived the study; K.D.K. performed developmental experiments; A.R.E. acquired three-dimensional data; K.D.K., A.R.E. and J.J. performed quantitative analyses; A.R.E. and J.J. constructed the model; A.R.E. performed computer simulations; K.D.K., A.R.E. and J.J. wrote the paper; and J.J. coordinated the study.

Author Information The three-dimensional scans for this study are deposited in the MorphoBrowser database, at http://morphobrowser.biocenter.helsinki.fi/. Reprints and permissions information is available at www.nature.com/reprints. The authors declare no competing financial interests. Correspondence and requests for materials should be addressed to K.D.K. (kathryn_kavanagh@yahoo.com) or J.J. (jernvall@fastmail.fm).

METHODS

Tooth cultures. Lower M1 tooth germs were dissected from heterozygous *ShhGFP* mouse *Shh*$^{tm1(EGFP/Cre)Cjt/+}$ embryos[33] at day 13 or 14 after fertilization and cultured at 37 °C and 5% CO_2 with a Trowell-type organ culture as described previously[30,34]. In brief, teeth were placed on 0.1 μm Nucleopore filter paper (Whatman) on a raised wire grid in a small Petri dish containing 2 ml of tissue medium (45% DMEM (Gibco), 45% F12/Glutamax (Gibco), 10% fetal bovine serum (PAA Laboratories GmbH) and 1% penicillin–streptomycin (10 U ml^{-1}; Gibco)]. Medium was replaced every two to three days, and ascorbic acid (100 μg ml^{-1}) was added. The epifluorescence of *ShhGFP* teeth closely follow the patterns of *Shh* expression detected with *in situ* hybridization techniques[28].

***In vitro* experiments.** Tooth germs were separated from the jaw tissue, which, if left in place, would grow and stunt the development of teeth in culture. Posterior tails of tooth germs in culture were separated from the tooth germ with a 25-gauge needle, and both pieces were cultured a short distance (about 100 μm) from each other on the same filter paper. For a clean cut, the filter paper with the tooth germ was briefly placed on a glass Petri dish for the cutting, taking care to avoid desiccation, then returned to the grid over medium. For day 13 tooth germs, the tail was cut from the point at which the initial anterior broadening stopped, or one-quarter of the way from the end of the tail. Digital images of 80 explants were taken daily (except for 80 out of 1,040 cases) from initiation to day 12 of culture under a fluorescence microscope (Leica MZFLIII microscope and Olympus DP50 digital camera system at magnifications of ×3.2 and ×4.0, resulting in 0.44 and 0.55 pixel μm^{-1} resolutions, respectively). Molar initiation date was tabulated by tracking backwards from the final M2 or M3 to the first visible epifluorescence marking the formation of the primary enamel knot.

Recombinant protein bead experiments were performed as described previously[30,34]. Agarose beads (Affi-Gel-Blue beads, catalogue no. 153-7302; Bio-Rad) were washed three times in PBS, then soaked in Activin A (100 ng μl^{-1})[50], BMP4 (100 ng μl^{-1}; R&D Systems) or BSA control (1 μg μl^{-1}; Sigma). Roughly 50 beads were soaked in 5 μl of 100 ng μl^{-1} protein solution for 45 min at 37 °C and a bead was placed with fine forceps on the posterior end of the day 14 tooth germ.

Quantitative analyses of experimental and macroevolutionary data. We chose the day 12 culture point for morphological measurements because at this stage M1 has reached, and M2 is close to reaching, asymptotic size and because after this day teeth are often difficult to measure accurately *in vitro* because of superfluous tissue growth and differentiation. From digital images we measured the two-dimensional areas of developing tooth crowns. Even when teeth have rolled onto their side this gives a reasonably consistent measure of size because cultured teeth have a tendency to flatten. However, explants in which M1 was pointing vertically, thus providing a considerable underestimate of its size relative to other molars, were excluded from measurements. The areas of 61 M1s, 48 M2s and 17 M3s were measured with NIH Image 1.63 and ImageJ (http://rsb.info.nih.gov/ij/). In addition, molar sizes were measured on alternate days of culture for 21 explants.

The 29 murine rodent species used in the macroevolutionary analysis were selected to represent the range of diets across the phylogeny within the subfamily and were determined from published literature sources described previously[42]. A tooth row of each species was scanned with a Nextec Hawk three-dimensional laser scanner and entered into the MorphoBrowser database at http://morphobrowser.biocenter.helsinki.fi/ (ref. 42). Teeth were oriented manually to maximize crown–base projection and crowns were captured with the JavaView viewing utility in MorphoBrowser. Two-dimensional areas were measured with NIH Image 1.63 and ImageJ. All ratios were plotted with the use of non-transformed mm^2 areas.

Developmental models. We assumed a linear effect of the activator and inhibitor ratio on tooth proportions, namely $(a - i)/i = (a/i) - 1$. Other relationships (for example, $\log(a/i)$) would alter the amount by which teeth changed along the inhibitory cascade trajectory but not the trajectory itself. Solving the molar sizes from $1 + [(a - i)/i](x - 1)$ gives M1 = 1, M2 = a/i and M3 = $2a/i - 1$. Molar proportions (of all the molars) are M1 = $i/3a$, M2 = 1/3 and M3 = $(2a - i)/3a$. From these formulae, the relationship between the M2/M1 ratio and the M3/M1 ratio is M3/M1 = 2(M2/M1) − 1. Note that the constant 1/3 proportion of M2 is lost if the tooth row has four molars. Progressively larger posterior molars may still be initiated sequentially if their growth rates are correspondingly faster. Even though the model may apply to volumes (or numbers of cells), we present our measurement data with two-dimensional surface areas because we consider these more reliable and because they are commonly used in morphological research. We note, however, that transforming the two-dimensional areas to volumes does not change the pattern of results. In the random relay model, we randomly reshuffled the M2/M1 sizes (in effect, the strength of $(a - i)/i$) before determining M3/M1 sizes. A total of 1,000 randomizations were performed in a custom Visual Basic 6.0 program and calculations of reduced major axis regressions were performed as described[49].

50. Harrington, A. E. *et al.* Structural basis for the inhibition of activin signalling by follistatin. *EMBO J.* **25**, 1035–1045 (2006).